Ceramics-Silikáty 70 (1), 25-33 (2026)
www.ceramics-silikaty.cz doi: 10.13168/cs.2025.0048

ISOTHERMAL CALORIMETRY DATABASE OF 65 CEMENTS WITH ANALYTICAL APPROXIMATIONS

[#]VÍT ŠMILAUER, JULIE EDELMANNOVÁ, PAVEL REITERMAN

Czech Technical University in Prague, Faculty of Civil Engineering, Thákurova 7, 166 29 Prague 6, the Czech Republic

[#]E-mail: vit.smilauer@cvut.cz

Submitted September 13, 2025, accepted October 22, 2025

Keywords: Isothermal calorimetry, Database, Released heat, Cement, Affinity hydration model, Exponential model

Isothermal calorimetry quantifies the heat flow of cementitious materials during hydration. The paper summarises the calorimetry results from 65 industrially produced cements manufactured between 2018-2025 in the central European region. The hydration proceeds under 20 °C, covering a wide range of Portland cements (CEM I), Portland-slag/limestone/composite cement (CEM II), blast furnace cement (CEM III), composite cements (CEM V), alkali-activated cement and sulfocalcic cement. The water/cement ratio was kept in a range of 0.40-0.50, the shortest measurement time took 237 h and the mean time was 421 h. Each cement is approximated with a four-parametric affinity hydration model with a standard deviation error as 4.11 J·g^{-1} and 11 selected cements are approximated with a simpler exponential model. The comprehensive database can serve for the prediction of the microstructure, mechanical properties, or temperature rise in massive concrete structures.

INTRODUCTION

The heat of cement hydration belongs to the basic properties of cement. It is widely used for the prediction of the temperature evolution and crack mitigation in massive concrete structures [1, 2, 3]. Liberated heat serves to quantify the effect of superplasticisers, shrinkage reducing admixtures [4], fly-ash [5], or sulfates [6] during the hydration of cement. The worldwide reduction of the clinker factor in recent years has given rise to a wide portfolio of new blended cements which have entered the sectors of construction, traffic and civil engineering. Generally, these blended cements alter the hydration kinetics and several construction steps require adjustments, e.g., formwork removal time, execution of post-tensioning, impact of the temperature, casting sequence of massive structures. This paper summarises the behaviour of 65 industrially produced cements from the central European region, supplying missing data on hydration kinetics.

The ratio between the released heat and the potential heat defines the overall degree of hydration of cement [7] which is used to estimate the compressive strength of concrete, Young's modulus, the basic creep, or the fracture energy [8]. In a more rigorous approach, the overall degree of hydration serves as a microstructure descriptor to quantify the volume fractions of the reacted cement, capillary porosity and hydration products [9], or to formulate and validate several hydration models for Portland and blended cements [7, 10, 11, 12]. The determination of the released heat has been standardised using the isothermal calorimetry method by ASTM C1702, ASTM C1679, or EN 196-11 and has started to replace the traditional heat-of-solution method.

It is well established that the temperature accelerates the heat release rate according to the Arrhenius equation. The apparent activation energy for various types of binders has been identified by isothermal calorimetry performed at different temperatures. The activation energy was found to vary within a very small range 40-42 kJ·mol^{-1} for two Portland cements and two oil-well cements [13]. Schindler [14] tested 20 Portland cements between Type I and V and found the apparent activation energy in a range of 37.3-50.0 kJ·mol^{-1}. Kada-Benameur et al. [15] found 38.3 kJ·mol^{-1} between 20-30 °C for CEM I 42.5 R. Barnett et al. [16] determined the activation energies for blended cements with ground granulated blast furnace slag; a 35 % replacement level led to 47 kJ·mol^{-1}, a 50 % replacement level led to 48 kJ·mol^{-1} and a 70 % replacement level led to 62.1 kJ·mol^{-1}. CEM III/A 42.5 N cement yielded 51.3 kJ·mol^{-1} [17].

The analysed cements were industrially manufactured during the years 2018-2025 in the central European region. Only limited data sets have been published so far, such as [14, 15, 16]. Published data sets usually focus on a few cements, laboratory-added admixtures or on the activation energy, however, data sets lack a wider range of cements manufactured industrially. Cement manufacturers in the central Europe tend to grind clinker and mineral admixtures together, which modifies the particle size distributions compared to the separate grinding often used in lab production. The database also contains cements with low a Blaine fineness from 250 $m^2 \cdot kg^{-1}$, ground in small quantities, which have excellent resistance to cracking during drying [18]. Each cement in the database is characterised by the type according to EN 197-1 [19], cement plant and Blaine fineness. The heat flow and heat release are later approximated by two empirical models; a four-parametric hydration model [20] and a two-parametric exponential model. The experimental data sets and both approximations can be found at the Zenodo repository https://doi.org/10.5281/zenodo.15212784.

Cements

Each cement in the database was manufactured during the years 2018-2025 and was classified according to EN 197-1 [19]. A detailed clinker analysis of approximately half of the cements revealed that the C_3S content fell in the range of 60-75 % and Na_2O_{eq} fell in the range of 0.45-0.80 %. Several coarsely ground cements in the database were made in small quantities by adjusting the grinding time. Two non-standard binders were added, particularly a commercially produced alkali-activated cement, called a H-cement [21], and a sulfocalcic cement [22]. The following list summarises the analysed cements in the database:

14 × CEM I (ordinary Portland cement),
12 × CEM II/A-S (Portland-slag cement),
2 × CEM II/A-LL (Portland-limestone cement),
1 × CEM II/A-M (Portland-composite cement),
22 × CEM II/B-S (Portland-slag cement),
1 × CEM II/B-LL (Portland-limestone cement),
2 × CEM II/B-M (Portland-composite cement),
1 × CEM II/C-M (Portland-composite cement),
4 × CEM III/A (Blast-furnace cement),
3 × CEM III/B (Blast-furnace cement),
1 × CEM V/A (Composite cement),
1 × H-cement (Alkali-activated cement),
1 × Sorfix (Sulfocalcic cement).

Isothermal calorimetry

Isothermal calorimetry was performed at 20 °C using a TamAIR calorimeter (Thermometric AB, Stockholm, Sweden, year 2007). Cement and water were mixed externally by hand for approximately 30 s and vibrated in an IKA Vortex I orbital shaker for 20 s. The external mixing brought the advantage of having complete control of the paste homogeneity and handling of sticky cements with high surface area. The procedure followed EN 196-11 method "A" for external mixing and approximately 18 g of the cement was used in each ampoule. Most of the measurements followed the prescribed w/c = 0.40 (39 cements), which was occasionally increased to 0.45 (24 cements) and 0.50 (2 cements), see Table 2 for the full details, and no cement was tested with two different w/c ratios.

The effect of increasing the w/c was studied by Lura et al. [23] who found that Portland cement showed a negligible difference in released heat up to 48 hours and gave 7 % more heat at 168 hours when the w/c was increased from 0.40 to 0.45. A similar result was found by Pang et al. [13], where the relative difference in the released heat was 7 % at 350 hours between a w/c 0.30 and 0.50. Increasing the w/c generally leads to higher kinetics at later ages due to the availability of water and less self-desiccation. External mixing yields a different temperature from a controlled temperature inside a calorimeter. Integrated heat flow right after the ampoule insertion contains a contribution from an unequilibrated temperature which plays a role up to approximately 0.75 hour. For this reason, the heat flow integration is separated into two parts:

- The liberated heat between 0-0.75 h is lumped into $Q_{0.75}$. The known initial temperature of a filled ampoule and the estimated thermal capacity were used in the calculation. The heat $Q_{0.75}$ contains a dominant contribution due to the dissolution of the cement and the initial hydration of the aluminates;
- The heat flow released after 0.75 h becomes integrated with zero initial heat. As a consequence, the degree of hydration at 0.75 hours is equal to zero.

The division of heat into two parts comes from an external mixing procedure that guarantees the proper homogenisation of the cement paste. Cement manufacturers often report the total liberated heat at 7 days, Q_{168}, which is included in Table 2 taking $Q_{0.75}$ into account. The shortest measurement took 237 h and the longest 941 h, the mean time is equal to 421 h, and the standard deviation is 143 h. Baseline calibration occurred prior to the test, and no calibration was performed after the measurement.

Approximation with the affinity hydration model

The affinity hydration model originates from the work of Ulm and Coussy [24]. The model was modified by introducing the affinity at the isothermal temperature of 25 °C. The rate of degree of hydration (DoH) yields

$$\frac{dDoH}{dt} = \tilde{A}_{25}(dDoH) \tag{1}$$

where the chemical affinity $\tilde{A}_{25}$ has a dimension of h^{-1}. The chemical affinity for the isothermal temperature can be obtained experimentally. Isothermal calorimetry measures the heat flow, $q(t)$, which, after integration, provides the hydration heat, $Q(t)$. The approximations under the isothermal 25 °C are given as

$$dDoH \approx \frac{Q(\mathrm{t})}{Q_{pot}} \tag{2}$$

$$\tilde{A}_{25}(DoH) \approx \frac{d}{dt}\left(\frac{Q(t)}{Q_{pot}}\right) = \frac{g(t)}{Q_{pot}} \tag{3}$$

where the potential (ultimate) heat of hydration, Q_{pot}, is expressed in J·g^{-1} of cement. It can be estimated from the mineral composition of the cement, e.g., the C_3S enthalpy yields 517 ±13 J·g^{-1} [25]. The potential heat and activation energy were assigned according to Table 1. The values correspond to the ranges found in the literature [13-17, 25-27].

Table 1. Assigned values for the potential heat and activation energy.

Cement type	Q_{pot} (J·g^{-1})	E_a (kJ·mol^{-1})
CEM I	500	38.3
CEM II/A-S, CEM II/A-LL, CEM II/A-M	460	40.0
CEM II/B-S, CEM II/B-LL, CEM II/B-M, CEM V/A	420	45.0
CEM II/C-M, Sorfix, H-cement	400	45.0
CEM III/A, CEM III/B	380	48.0

Cervera et al. [28] proposed an analytical form of the normalised affinity which was refined later [29]. A slightly modified formulation was adopted here [20]

$$\begin{aligned}\tilde{A}_{25}(DoH) = B_1\left(\frac{B_2}{DoH_\infty} + DoH\right)\cdot \\ \cdot\,(DoH_\infty - DoH)\exp\left(-\bar{\eta}\,\frac{DoH}{DoH_\infty}\right)\end{aligned} \tag{4}$$

where B_1, B_2 are coefficients to be calibrated, DoH_∞ is the ultimate hydration degree and $\bar{\eta}$ represents the microdiffusion of free water through the formed hydrates. The parameters in Equation (4) express isothermal hydration at 25 °C. When the hydration proceeds under a different temperature, the Arrhenius equation scales the affinity to an arbitrary temperature T

$$\tilde{A}_T = \tilde{A}_{25}\exp\left[\frac{E_a}{R}\left(\frac{1}{273.15+25} - \frac{1}{T}\right)\right] \tag{5}$$

$$t_e = t\exp\left[\frac{E_a}{R}\left(\frac{1}{273.15+25} - \frac{1}{T}\right)\right] \tag{6}$$

where t_e is an equivalent time corresponding to a reference temperature 25 °C, T is the arbitrary constant temperature of hydration, R is the universal gas constant (8.314 Jmol^{-1}K^{-1}) and E_a is the apparent activation energy.

The affinity function in Equation (4) needs to be integrated numerically by sufficiently small, time increments. The predictor-corrector scheme is implemented into the form

$$DoH_0^{(1)} = DoH^{(0)} + \tilde{A}_T(DoH^{(0)})\cdot\Delta t \tag{7}$$

$$DoH_{n+1}^{(1)} = DoH^{(0)} + [\tilde{A}_T(DoH^{(0)}) + \tilde{A}_T(DoH_n^{(1)})]\cdot\frac{\Delta t}{2} \tag{8}$$

Three iterations usually suffice, so that n = 0, 1, 2. The released heat up to 0.75 h is lumped into $Q_{0.75}$. The numerical evaluation of Equations (7) and (8) normally starts at t = 0.75 h where it is assumed that DoH = 0. In several cases, the heat flow integration started later, between 0.8-2.3 h. Those datasets are marked in Table 2 and $Q_{0.75}$ is estimated.

Each experimental data set was sampled at 300 time points, which were equally distributed on the log time from the beginning to the end of the measurements. Python's function curve_fit, from the scipy.optimize module, found three parameters of the affinity hydration model within the ranges of $B_1 \in [0.1, 3]$ h^{-1}, $B_2 \in [10^{-8}, 10^{-2}]$ and $\eta \in [4, 14]$. Only three cements required to restrain the parameters even more to obtain a more reasonable fit. The parameter DoH_∞ = 0.85 was assumed for all the cement pastes which have a $w/c \in [0.40, 0.50]$.

Approximation with the exponential hydration model

A three-parametric equation has been suggested by Freiesleben, Hansen and Pedersen [30] for the strength estimate. The equation was adopted for released heat as

$$Q(t) = Q_{\mathrm{pot}}\,DoH_\infty\exp\left[-\left(\frac{\tau}{t}\right)^\beta\right] \tag{9}$$

with the parameters τ, β.

RESULTS AND DISCUSSION

The degree of hydration, the potential hydration heat, and the released heat are bound by Equation (2). First, the potential heat and activation energies were estimated based on the cement class, see Table 1. Second, the asymptotic degree of hydration was assumed as DoH_∞ = 0.85 for all the cements due to missing long-term measurements. A one-year study at a w/c = 0.40 and CEM I revealed a maximum DoH = 0.826 by means of X-ray diffraction (XRD)-Rietveld and isothermal calorimetry [5] that is close to the selected asymptotic value. The assumption that DoH_∞ = 0.85 has an impact on the fitted model parameters and the predicted DoH. According to Equation (2), the only condition $DoH_\infty \geq Q(t_{\max})/Q_{\mathrm{pot}}$ is valid for all the tests up to 237 h and likely to one-year as tested above by the XRD-Rietveld analysis [5]. Blended cements with slag or fly ash exhibited lower values for the degree of hydration at 90 days by thermogravimetry [31] which would require lowering the DoH_∞. The situation changes when long times above one year should be analysed; if w/c ≥ 0.42 in CEM I, the hydration may proceed to complete hydration, requiring a DoH_∞ = 1 [32, 33]. Better estimations of DoH and DoH_∞ for cements would need complementary methods

Table 2. Properties of the cements and parameters for the affinity hydration model.

Cement name - Blaine fineness	EN 197-1	w/c	B_1 (h^{-1})	B_2	$\bar{\eta}$	Q_{pot} (J·g⁻¹)	$Q_{0.75}$ (J·g⁻¹)	Q_{168} (J·g⁻¹)	E_a (kJ·mol⁻¹)
114-CEM I 32.5 R Ladce - 250a	CEM I	0.45	0.495	3.43e-3	8.38	500	12.0b	249	38.3
103-CEM I 42.5 Rsc Mokra - 256a	CEM I	0.45	0.652	2.49e-3	7.73	500	12.0b	279	38.3
179-CEM I 42.5 Rsc Mokra - 263	CEM I	0.40	0.685	2.92e-3	6.95	500	19.0	313	38.3
106-CEM I 42.5 N Mokra - 264a	CEM I	0.45	0.638	4.53e-3	6.82	500	12.0b	305	38.3
105-CEM I 42.5 Rsc Mokra - 306a	CEM I	0.45	0.785	2.67e-3	6.90	500	12.0b	312	38.3
158-CEM I 42.5 Rsc Mokra - 312	CEM I	0.40	0.964	3.56e-4	7.42	500	9.3	305	38.3
109-CEM I 42.5 Rsc Mokra - 320a	CEM I	0.45	0.730	1.90e-3	7.13	500	12.0b	302	38.3
100-CEM I 32.5 R Ozarow - 330a	CEM I	0.45	0.567	4.08e-3	6.78	500	10.0b	298	38.3
115-CEM I 42.5 R Ladce - 339a	CEM I	0.45	0.879	1.10e-3	7.62	500	12.0b	304	38.3
163-CEM I 42.5 Rsc Hranice - 340	CEM I	0.45	0.916	9.76e-4	6.17	500	4.5	337	38.3
172-CEM I 42.5 R Rohoznik - 390	CEM I	0.40	1.417	1.84e-4	8.64	500	11.0	291	38.3
122-CEM I 52.5 R Cizkovice - 397a	CEM I	0.50	1.283	9.27e-4	5.67	500	12.0b	375	38.3
202-CEM I 42.5 R Mokra - 409	CEM I	0.40	1.424	4.21e-5	7.85	500	9.5	298	9.5
116-CEM I 52.5 R Ladce - 415a	CEM I	0.45	1.078	1.37e-3	7.17	500	12.0b	325	38.3
148-CEM-II-A-S 42.5 N Mokra - 307	CEM II/A-S	0.40	0.870	5.17e-4	7.00	460	11.0	291	40.0
108-CEM II-A-S 42.5 N Mokra - 310a	CEM II/A-S	0.45	0.699	2.41e-3	7.22	460	10.0b	269	40.0
147-CEM-II-A-S 42.5 N Mokra - 315	CEM II/A-S	0.40	1.320	1.50e-5	8.05	460	11.1	288	40.0
196-CEM II-A-S 42.5 Nsc Mokra - 319	CEM II/A-S	0.40	0.659	2.38e-3	6.87	460	10.4	280	40.0
135-CEM II-A-S 42.5 R Cizkovice - 340	CEM II/A-S	0.40	1.072	1.91e-3	5.78	460	23.7	349	40.0
188-CEM II-A-S 42.5 N Mokra - 343	CEM II/A-S	0.40	0.591	3.58e-3	6.53	460	18.0	287	40.0
193-CEM II-A-S 42.5 N Ladce - 344	CEM II/A-S	0.40	0.725	8.13e-4	7.93	460	4.7	254	40.0
146-CEM-II-A-S 42.5 N Mokra - 361	CEM II/A-S	0.40	0.990	4.34e-4	7.62	460	8.8	279	40.0
131-CEM II-A-S 42.5 R Prachovice - 365	CEM II/A-S	0.40	1.068	5.85e-4	6.42	460	14.9	316	40.0
107-CEM II-A-S 42.5 N Mokra - 388a	CEM II/A-S	0.45	0.779	1.97e-3	7.13	460	10.0b	278	40.0
195-CEM II-A-S 42.5 R Ladce - 434	CEM II/A-S	0.40	1.119	2.66e-4	7.91	460	7.9	281	40.0
180-CEM II-A-S 42.5 R Mokra - 457	CEM II/A-S	0.40	0.839	6.89e-4	6.41	460	11.5	305	40.0
165-CEM II-A-LL 42.5 R Hranice - 423	CEM II/A-LL	0.45	0.625	3.87e-3	5.95	460	6.1	303	40.0
186-CEM II-A-LL 42.5 R Radotin - 460	CEM II/A-LL	0.40	1.026	5.28e-4	6.62	460	21.6	320	40.0
197-CEM II-A-M (S-V) 42.5 R Prachovice - 383	CEM II/A-M	0.40	1.000	1.53e-3	6.27	460	8.2	313	40.0
152-CEM-II-B-S 32.5 R Mokra - 317	CEM II/B-S	0.40	0.655	3.41e-3	6.29	420	7.8	266	45.0
151-CEM-II-B-S 32.5 R Mokra - 324	CEM II/B-S	0.40	0.798	2.13e-3	6.83	420	7.7	262	45.0
137-CEM-II-B-S 32.5 R Cizkovice - 325	CEM II/B-S	0.40	0.916	1.79e-3	5.95	420	13.8	296	45.0
153-CEM-II-B-S 32.5 R Radotin - 326	CEM II/B-S	0.40	0.842	8.62e-4	6.80	420	8.8	267	45.0
155-75%CEM I 42.5 Rsc Mokra - 306+25%SMS400 - 330a	CEM II/B-S	0.45	0.525	6.27e-3	6.24	420	10.0b	261	45.0
181-CEM II-B-S 32.5 R Mokra - 331	CEM II/B-S	0.40	0.616	2.74e-3	6.76	420	13.0	254	45.0
189-CEM II-B-S 32.5 R Mokra - 331	CEM II/B-S	0.40	0.671	3.46e-3	7.17	420	8.0	245	45.0
110-75%CEM I 42.5 Rsc Mokra+25%SMS400 - 340a	CEM II/B-S	0.45	0.523	6.31e-3	6.24	420	10.0b	261	45.0
118-CEM II-B-S 32.5 R Prachovice - 343a	CEM II/B-S	0.45	1.138	5.07e-5	7.32	420	10.0b	267	45.0
134-CEM II-B-S 32.5 R Prachovice - 343	CEM II/B-S	0.40	0.985	3.29e-4	6.55	420	18.4	281	45.0
111-70%CEM I 42.5 Rsc Mokra - 306+30%SMS400 - 344a	CEM II/B-S	0.45	0.464	7.25e-3	6.31	420	10.0b	252	45.0
156-70%CEM I 42.5 Rsc Mokra - 306+30%SMS400 - 344a	CEM II/B-S	0.45	0.465	7.19e-3	6.32	420	10.0b	252	45.0
101-75%CEM I 32.5 R Ozarow - 330+25%SMS 400 - 348a	CEM II/B-S	0.45	0.417	1.00e-2	6.11	420	10.0b	249	45.0
173-CEM-II-B-S 42.5 N Hranice - 351	CEM II/B-S	0.40	0.703	3.21e-3	6.60	420	10.0	266	45.0
159-CEM-II-B-S 32.5 R Mokra - 358	CEM II/B-S	0.40	0.735	2.11e-3	6.50	420	5.8	264	45.0
160-CEM-II-B-S 32.5 R Mokra - 371	CEM II/B-S	0.40	0.711	2.40e-3	6.52	420	7.2	263	45.0
149-CEM-II-B-S 32.5 R Mokra - 380	CEM II/B-S	0.40	0.925	1.25e-3	6.90	420	9.4	268	45.0
136-CEM II-B-S 42.5 N Cizkovice - 385	CEM II/B-S	0.40	1.073	1.34e-3	6.04	420	19.4	306	45.0
132-CEM II-B-S 42.5 R Kiralyegyhaza - 410	CEM II/B-S	0.40	1.066	4.60e-4	6.39	420	12.7	285	45.0
198-CEM II-B-S 32.5 R Mokra - 413	CEM II/B-S	0.40	0.928	9.42e-4	7.44	420	5.7	254	45.0
161-CEM-II-B-S 32.5 R Mokra - 423	CEM II/B-S	0.40	0.884	1.42e-3	6.74	420	7.8	267	45.0
102-CEM II-B-S 32.5 R Mokra - 433a	CEM II/B-S	0.45	0.738	1.56e-3	7.42	420	10.0b	243	45.0
167-CEM II-B-LL 32.5 R Hranice - 488	CEM II/B-LL	0.45	0.544	3.40e-3	6.21	420	4.3	255	45.0
187-CEM II-B-M (S-LL) 42.5 N Radotin - 391	CEM II/B-M	0.40	0.817	9.46e-4	6.69	420	16.0	275	45.0
182-CEM II-B-M (S-LL) 42.5 N Hranice - 403	CEM II/B-M	0.40	0.849	1.93e-3	6.30	420	16.1	288	45.0
183-CEM II-C-M (S-LL) 42.5 N Hranice - 450	CEM II/C-M	0.40	0.979	1.39e-3	6.57	400	16.5	273	47.0
157-50%CEM I 42.5 Rsc - 306 Mokra+50%SMS400 - 353a	CEM III/A	0.45	0.419	1.00e-2	6.79	380	10.0b	210	48.0
119-75%CEM II-B-S 32.5 R Prach.+25%SMS400 - 357a	CEM III/A	0.45	0.732	1.06e-3	7.03	380	10.0b	229	48.0
112-50%CEM I 42.5 Rsc Mokra+50%SMS 400 - 360a	CEM III/A	0.45	0.419	1.00e-2	6.79	380	10.0b	210	48.0
184-CEM III-A 42.5 N Hranice - 408	CEM III/A	0.40	0.715	2.88e-3	6.69	380	15.7	241	48.0
201-CEM III-B 32.5 N LH-SR Prachovice - 338	CEM III/B	0.40	0.480	4.23e-3	8.16	380	4.2	182	48.0
199-CEM III-B 32.5 L-LH Mokra - 462	CEM III/B	0.40	0.714	1.91e-3	8.50	380	6.7	195	48.0
121-CEM III-B - 32.5 N LH-SR Mokra - 495a	CEM III/B	0.45	0.280	1.00e-2	6.96	380	8.0b	186	48.0
200-CEM V-A (S-V) 32.5 R Prachovice - 444	CEM V/A	0.40	1.056	2.46e-4	8.46	420	7.2	235	45.0
174-H-cement 32.5 R – 610	H-cement	0.40	2.000	4.58e-4	10.52	400	14.0	211	45.0
162-Sorfix – 1011	Sorfix	0.50	0.588	1.00e-2	6.42	400	17.4	262	45.0

Notes:

a – integration started between 0.8-2.3 hours of hydration; b – estimated values such as XRD or thermogravimetry. Altering $DoH_\infty \neq 0.85$ requires recalibration of the model parameters from the experimental data. Then, the prediction within calibrated data will be similar, however, caution should be taken with the year-long lasting predictions for various purposes.

The initial released heat $Q_{0.75}$ was measured in the range 4.5-23.7 J·g^{-1} for 43 cements, following the procedure described in Section 3. The rest of the 22 cements estimated this value from similar cements. Weak correlation was found depending on the cement plant, likely reflecting the clinker composition, sulfate dosage, grinding aids, residuals from alternative fuels or alkali availability during the initial hydration [34].

Approximations with the affinity hydration model

Table 2 summarises the cement description, manufacturer, Blaine fineness, strength class, *w*/*c* and parameters for the affinity hydration model. The table includes eight binary systems, where CEM I or CEM II was intermixed with a ground granulated blast furnace slag SMS with the Blaine fineness of 400 m^2·kg^{-1}. The fitting of 65 cements led to the ranges for $B_1 \in [0.28,\ 2.0]$ h^{-1}, $B_2 \in [1.5\times10^{-5},\ 1.0\times10^{-2}]$ and $\overline{\eta} \in [5.67,\ 10.52]$. The parameter B_1 controls the overall hydration rate and is important for the length of the dormant period. Indeed, the correlation coefficient with the two-day compressive strength is equal to 0.62. B_2 controls the middle-age kinetics and the long-term kinetics. The correlation coefficient of –0.28 between B_2 and $\tilde{\eta}$ shows that the parameters are rather independent.

Figure 1 shows the heat flow for the CEM I cements where the solid lines represent the experimental data and the dots represent the affinity hydration model. Cement dissolution, early ettringite and C–S–H formation occur during the induction period, taking place up to approximately 2 hours. External mixing leads to higher initial temperature, usually in the range 20-24 °C, which also contributes to the early heat flow through temperature equilibration. Low heat flow is noticeable during the induction period, approximately between 2-4 hours, followed by the accelerating period with the peak between 8-11 hours. The rest of the hydration falls in the decelerating period. The sulfate depletion local peak, noticeable at around 20 hours, reflects the faster precipitation of ettringite and higher dissolution of C_3A. The last local peak, after 20 hours, signals the formation of AFm [35].

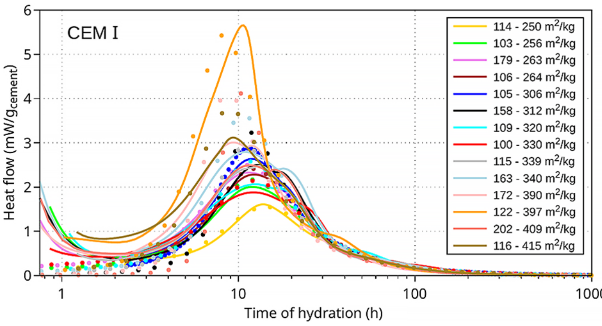

Figure 1. Heat flow from the CEM I cements (solid lines = calorimetry, dots = affinity model).

Figure 2 shows the released heat for the CEM I types. As stated above, the integration normally started at 0.75 h and, in some cases, up to 2.3 h, see the note in Table 2. The fitting algorithm for the released heat uses the least-squares method, where each of the 300 points share the same weight. The derivative represents the heat flow and the fit is generally worse.

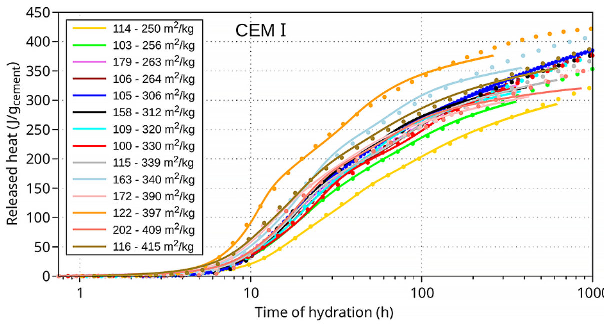

Figure 2. Released heat from the CEM I cements (solid lines = calorimetry, dots = affinity model).

The heat released in Figure 3 demonstrates the behaviour of the CEM II/A cements with the slag, limestone, or other constituents. The cements contain at least 80 % of the clinker. Figures 4 and 5 cover the Portland-slag cement CEM II/B-S with at least 65 % of the clinker.

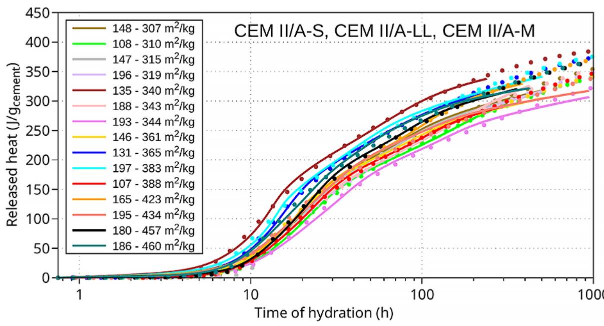

Figure 3. Released heat from the CEM II/A-S, CEM II/A-LL, CEM II/A-M cements.

The Portland-limestone cements CEM II/B-LL and the Portland-composite cements CEM II/B-M, CEM II/C-M are displayed in Figure 6. These cements contain at least 50 % of the clinker. The blast-furnace cement CEM III/A, CEM III/B and composite cement CEM V/A contain 20-64 % of the clinker, see Figure 7. They have the lowest heat release and are suitable candidates for massive concrete structures.

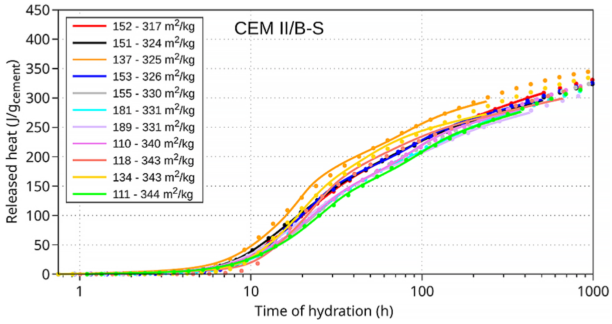

Figure 4. Released heat from the CEM II/B-S cements below 344 $m^2 \cdot kg^{-1}$.

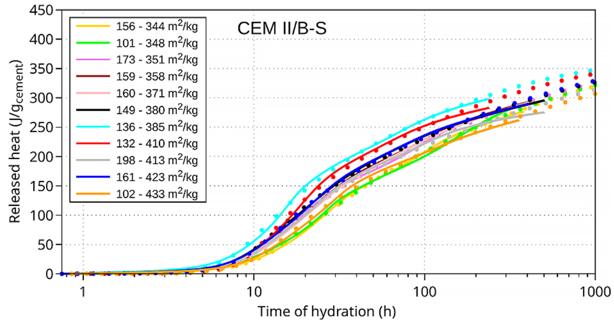

Figure 5. Released heat from the CEM II/B-S cements above 344 $m^2 \cdot kg^{-1}$.

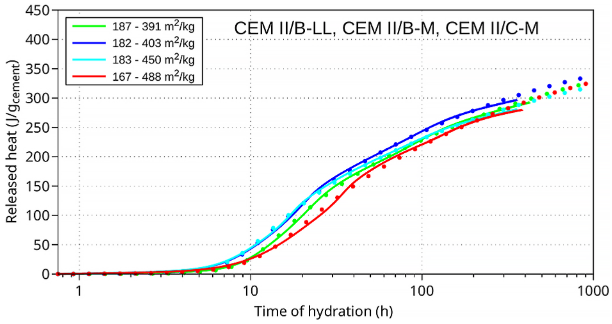

Figure 6. Released heat from the CEM II/B-LL, CEM II/B-M, CEM II/C-M cements.

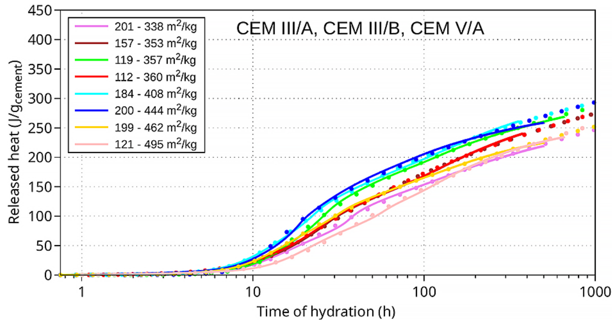

Figure 7. Released heat from the CEM III/A, CEM III/B, CEM V/A cements.

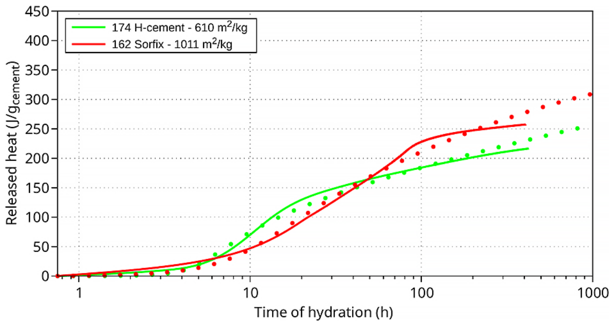

Figure 8. Released heat from the Sorfix and H-cement.

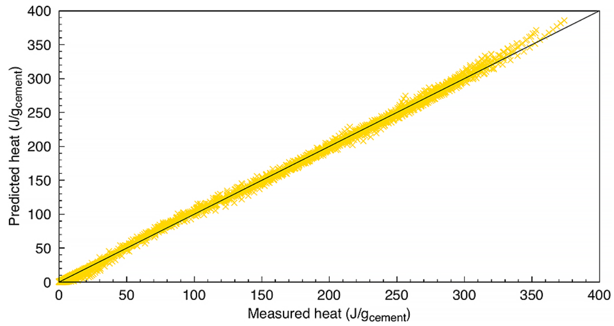

Figure 9. Validation of the released heat with the affinity hydration model.

Two special cements, industrially produced in limited amounts, are covered in Figure 8. Sorfix represents a sulfocalcic cement made completely without Portland clinker taking advantage of the controlled ettringite formation and C–S–H [22, 36]. An alkali-activated hybrid cement, called H-cement, contains 20 % of the Portland clinker and the reactivity is promoted by alkalies [21, 37]. The fitted curves show the inability to capture local peaks which are likely caused by the massive ettringite formation and alkali activation process.

Figure 9 shows an excellent fit for the affinity hydration model in terms of the released heat for all the cements. Pearson's correlation coefficient yields 0.9994. The small underestimate of the long-term released heat (after approximately 3 weeks) becomes notable for many cements; this behaviour possibly stems from the evaporation of water from imperfectly sealed ampoules.

Approximations with the affinity hydration model

Eleven common cements were selected and approximated with the exponential model according to Equation (9), see Table 3. The asymptotic degree of hydration was set again as $DoH_\infty = 0.85$ for all the cements.

Figure 10 displays the released heat with the fits. The exponential model performs slightly worse in fitting the experimental data. Heat up to 50 $J \cdot g^{-1}$ is rather over-predicted and rather under-predicted in the range of 100-200 $J \cdot g^{-1}$, see Figure 11. Pearson's correlation coefficient reaches 0.9972 from all 65 cements.

Coefficient of variation of the error

The deviations between the fitted model and the released heat can be quantified by the coefficient of variation of the error [38]. The standard error for large data sets reads:

$$s = \sqrt{\frac{1}{n}\sum_{i=1}^{n}(y_i - Y_i)^2} \tag{10}$$

where n is the number of data points from all the data sets, y_i contains isothermal calorimetry data and Y_i is the corresponding model prediction. The time is sampled to 300 points distributed equally on the log axis which was found to be sufficient. The weighted mean of all the sampled values is equal to

$$\bar{y} = \frac{1}{n}\sum_{i=1}^{n} y_i \tag{11}$$

and the coefficient of variation (CoV) over all the data yields

$$\omega = \frac{s}{\bar{y}} \tag{12}$$

For the affinity hydration model and all 65 cements, the standard deviation of the error yields s = 4.11 J·g^{-1}, the mean value is y = 114.8 J·g^{-1} (at 68.1 h) and the coefficient of variation is ω = 0.036. The exponential model provides approximately a two-times larger error, i.e., s = 8.62 J·g^{-1} and ω = 0.075.

Effect of the temperature and admixtures

When the hydration proceeds above 20 °C, the equivalent time runs faster and the experimental data span a shorter interval. The average measurement period for 65 pastes took 421 h. In such a case, a constant temperature, e.g., 60 °C and an activation energy of 40 kJ·mol^{-1} shorten the covered time to 421/7.17 = 58.7 h. Beyond this time, the affinity/exponential hydration models extrapolate beyond the measured data, introducing more uncertainty to the results. This situation occurs quite often by simulating massive concrete elements that cool for several weeks [2].

The data sets characterise the plain cement pastes without any admixtures. Concrete usually contains a plasticiser that has an impact on the heat flow, usually causing the prolongation of the dormant period and the flattening of the peaks [39]. The effect of retarders and accelerators is even more pronounced. The accurate analysis of admixture-rich concretes requires performing direct experiments and published data sets for plain pastes provide only a rough guideline.

CONCLUSIONS

The paper summarises the heat released from 65 industrially produced cements from the region of central Europe, in which several have appeared recently. Isothermal calorimetry at 20 °C was used with an external mixing procedure. The data sets span the range from Portland CEM I, blended CEM II/III to composite CEM V cements, addressing many concretes used in civil engineering and infrastructure projects.

Table 3. Parameters for the exponential hydration model.

Cement name - fineness	EN 197-1	w/c	τ (h)	β	Q_{pot} (J/g)
109-CEM I 42.5 Rsc Mokra - 320a	CEM I	0.45	33.0	0.627	500
100-CEM I 32.5 R Ozarow - 330a	CEM I	0.45	35.7	0.625	500
122-CEM I 52.5 R Cizkovice - 397a	CEM I	0.50	15.8	0.871	500
107-CEM II-A-S 42.5 N Mokra - 388a	CEM II/A-S	0.45	33.2	0.656	460
165-CEM II-A-LL 42.5 R Hranice - 423	CEM II/A-LL	0.45	27.8	0.720	460
173-CEM-II-B-S 42.5 N Hranice - 351	CEM II/B-S	0.40	30.1	0.653	420
167-CEM II-B-LL 32.5 R Hranice - 488	CEM II/B-LL	0.45	35.0	0.692	420
183-CEM II-C-M (S-LL) 42.5 N Hranice - 450	CEM II/C-M	0.40	24.0	0.694	400
184-CEM III-A 42.5 N Hranice - 408	CEM III/A	0.40	31.1	0.650	380
199-CEM III-B 32.5 L-LH Mokra - 462	CEM III/B	0.40	48.1	0.513	380
200-CEM V-A (S-V) 32.5 R Prachovice - 444	CEM V/A	0.40	37.1	0.554	420

Notes: a – integration started between 0.8-2.3 hours of hydration.

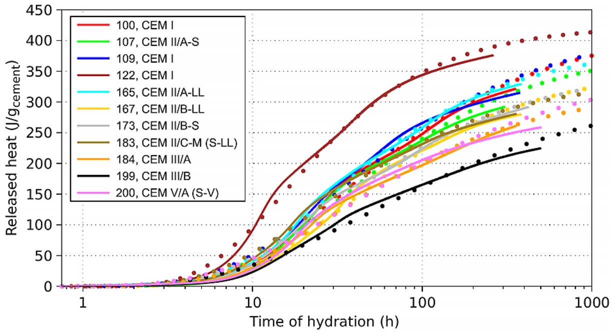

Figure 10. Released heat from 11 cements.

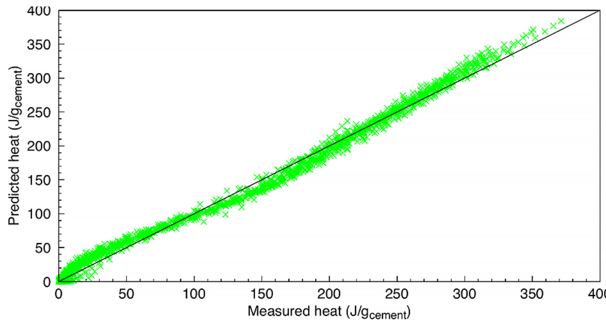

Figure 11. Validation of the released heat with the exponential hydration model.

The affinity and exponential hydration models were calibrated to the experimental data with the coefficient of variation of the error as 3.6-7.5 %. The approximations can be used to estimate the degree of hydration, microstructure evolution, mechanical properties, temperature rise, or risk of thermal cracking. The experimental data sets with the approximations were uploaded to the Zenodo repository https://doi.org/10.5281/zenodo.15212784.

Acknowledgements

This research was supported by the Czech Science Foundation, grant number 25-16766S (methodology, calorimetry). The cement supply and industrial collaboration was supported by the Technology Agency of the Czech Republic, grant number TS01030114. Cement producers are acknowledged for fruitful collaboration.

REFERENCES

1. Waller V., Larrard F. de, Roussel P. (1996): Modelling the temperature rise in massive HPC structures. in: *Fourth international symposium on utilization of high-strength/high-performance concrete,* RILEM, 415–421.
2. Fairbairn E. M. R., Azenha M., Asamoto S., Ballim Y., Benboudjema F., Briffaut M., Carette J. et al. (2019). *Thermal Cracking of Massive Concrete Structures.* RILEM State-of-the-art reports. Springer.
3. Do T. A., Hoang T. T., Bui-Tien T., Hoang H. V., Do T. D., Nguyen P. A. (2020): Evaluation of heat of hydration, temperature evolution and thermal cracking risk in high-strength concrete at early ages. *Case Studies in Thermal Engineering, 21*, 100658. doi: 10.1016/j.csite.2020.100658
4. Kiernożycki W. (2019): Calorimetric measurements and numerical modelling of the effects of selected chemical admixtures on the development of cement hydration at different temperatures. *Cement-Wapno-Beton (Cement-Lime-Concrete), 24*, 432–447.
5. Linderoth O., Wadsö L., Jansen D. (2021): Long-term cement hydration studies with isothermal calorimetry. *Cement and Concrete Research, 141*, 106344. doi: 10.1016/j.cemconres.2020.106344
6. Sandberg P., Bishnoi S. (2018): Sulphate Optimization of Binders with Calcined Clay Using Isothermal Calorimetry. In Martirena F., Favier A. and Scrivener K. (eds): *Calcined Clays for Sustainable Concrete*. Dordrecht: Springer Netherlands, 422–426. doi: 10.1007/978-94-024-1207-9_68
7. van Breugel K. (1991): Simulation of Hydration and Formation of Structure in Hardening Cement-based Materials. Ph.D. Thesis, TU Delft.
8. De Schutter G., Taerwe L. (1996): Degree of hydration-based description of mechanical properties of early age concrete. *Materials and Structures, 29,* 335–344. doi: 10.1007/BF02486341
9. Brouwers H. (2004): The work of Powers and Brownyard revisited: Part 1. *Cement and Concrete Research, 34*, 1697 – 1716. doi: 10.1016/j.cemconres.2004.05.031
10. Bentz D. P. (2000): CEMHYD3D: A Three-Dimensional Cement Hydration and Microstructure Development Modeling Package. Version 2.0. Tech. Rep., NIST Building and Fire Research Laboratory, Gaithersburg, Maryland. doi: 10.6028/NIST.IR.5977
11. Thomas J. J., Biernacki J. J., Bullard J. W., Bishnoi S., Dolado J. S., Scherer G. W., Luttge A. (2011): Modeling and simulation of cement hydration kinetics and microstructure development. *Cement and Concrete Research, 41*, 1257–1278. doi: 10.1016/j.cemconres.2010.10.004
12. Zhang L.-N., Sun F., Liu Y., Lee S. and Wang X.-Y. (2024): A numerical hydration model to predict the macro and micro properties of cement–eggshell powder binary blends. *Applied Sciences, 14*, doi:10.3390/app14135775
13. Pang X., Sun L., Sun F., Zhang G., Guo S., Bu Y. (2021): Cement hydration kinetics study in the temperature range from 15 °C to 95 °C. *Cement and Concrete Research, 148*, doi:10.1016/j.cemconres.2021.106552
14. Schindler A. K. (2004): Effect of temperature on hydration of cementitious materials. ACI *Materials Journal 101*, 72–81. doi: 10.14359/12990
15. Kada-Benameur H., Wirquin E. and Duthoit B. (2000): Determination of apparent activation energy of concrete by isothermal calorimetry. *Cement and Concrete Research, 30,* 301–305. doi: 10.1016/S0008-8846(99)00250-1
16. Barnett S., Soutsos M., Millard S., Bungey J. (2006): Strength development of mortars containing ground granulated blast-furnace slag: Effect of curing temperature and determination of apparent activation energies. *Cement and Concrete Research, 36*, 434–440. doi: 10.1016/j.cemconres.2005.11.002
17. Kiernożycki W., Blyszko J. (2021): The influence of temperature on the hydration rate of cements based on calorimetric measurements. *Materials, 14,* 3025. doi: 10.3390/ma14113025
18. Šmilauer V., Reiterman P., Šulc R., Schořík P. (2022): Crack-resistant cements under drying: Results from ring shrinkage tests and multi-physical modeling. *Materials, 15*, 4040. doi: 10.3390/ma15124040
19. CEN/TC 51 committee (2011): Cement – Part 1: Composition, specifications and conformity criteria for common cements. Standard, Comite Europeen de Normalisation.
20. Da Silva W. R. L., Šmilauer V., Štemberk P. (2015): Upscaling semi-adiabatic measurements for simulating temperature evolution of mass concrete structures. *Materials and Structures, 48,* 188–197. doi: 10.1617/s11527-013-0213-3
21. Šmilauer V., Dohnalová L., Martauz P. (2024): Shrinkage and creep properties of low-carbon hybrid cement. *Materials, 17*,4417. doi:10.3390/ma17174417
22. Škvára F., Šulc R., Snop R., Peterová A.,Šídlová M. (2018): Hydraulic clinkerless binder on the fluid sulfocalcic fly ash basis. *Cement and Concrete Composites, 93*, 118–126, doi: 10.1016/j.cemconcomp.2018.06.020
23. Lura P., Winnefeld F., Fang X. (2017). A simple method for determining the total amount of physically and chemically bound water of different cements. *Journal of Thermal Analysis and Calorimetry, 130*, 653-660, doi: 10.1007/s10973-017-6513-z
24. Ulm F.-J., Coussy O. (1995): Modeling of thermochemomechanical couplings of concrete at early ages. *Journal of Engineering Mechanics, 121*, 785–794, doi: 10.1061/(ASCE)0733-9399(1995)121:7(785)
25. Taylor H. F. W. (1990). *Cement Chemistry*. Academic Press, New York.
26. Bentz D. P. (2007): Verification, Validation, and Variability of Virtual Standards. In Beaudoin J. J., Makar J. M. and

Raki L. (eds), *12th International Congress on the Chemistry of Cement*.
27. Czernin W. (1980). *Cement Chemistry and Physics for Civil Engineers*. Bauverlag GmbH, Wiesbaden und Berlin, 2nd ed.
28. Cervera M., Oliver J., Prato T. (1999): Thermo-chemo-mechanical model for concrete. I: Hydration and aging. *Journal of Engineering Mechanics ASCE* 125, 1018–1027. doi: 10.1061/(ASCE)0733-9399(1999)125:9(1018)
29. Gawin D., Pesavento F., Schrefler B. A. (2006): Hygro-thermo-chemo-mechanical modelling of concrete at early ages and beyond. Part I: Hydration and hygro-thermal phenomena. *International Journal for Numerical Methods in Engineering, 67*, 299–331. doi: 10.1002/nme.1615
30. Hansen P. F.,Pedersen E. (1984). *Curing of concrete structures*. Lyngby, Denmark: BKI.
31. Reiterman P., Holčapek O., Davidová V., Jaskulski R., Keppert M. (2019). Estimation of hydration degree of blended cements with the help of k-values. *Materials, 12*, 2420. doi: 10.3390/ma12152420
32. Hansen T. C. (1986): Physical structure of hardened cement paste. A classical approach. *Matèriaux et Constructions* 114, 423–436. doi:10.1007/BF02472146
33. Rahimi-Aghdam S., Bažant Z. P., Abdolhosseini Qomi M. (2017): Cement hydration from hours to centuries controlled by diffusion through barrier shells of C–S–H. *Journal of the Mechanics and Physics of Solids, 99*, 211–224, doi:10.1016/j.jmps.2016.10.010
34. Chen J., Jia J., Zhu M. (2024): Understanding the effect of alkali content on hydration, hardening, and performance of Portland cement – a comprehensive review. *Materials Today Communications,* 40, 109728. doi: 10.1016/j.mtcomm.2024.109728
35. Marchon D., Flatt R. (2016): 8 – mechanisms of cement hydration. In Aïtcin P.-C. and Flatt R. J. (eds), *Science and Technology of Concrete Admixtures*. Cambridge: Elsevier, 129–145, doi: 10.1016/B978-0-08-100693-1.00008-4
36. Hlaváček P., Šulc R., Šmilauer V., Rößler C., Snop R. (2018): Ternary binder made of CFBC fly ash, conventional fly ash, and calcium hydroxide: Phase and strength evolution. *Cement and Concrete Composites, 90*, 100–107, doi: 10.1016/j.cemconcomp.2017.09.020
37. Martauz P., Janotka I., Strigáč J., Bačuvčík M. (2016): Fundamental properties of industrial hybrid cement: utilization in ready mixed concretes and shrinkage-reducing applications. *Materiales de Construcción, 66*, 1–14. doi:10.3989/mc.2016.04615
38. Wendner R., Hubler M. H., Bažant Z. P. (2015): Optimization method, choice of form and uncertainty quantification of model B4 using laboratory and multi-decade bridge databases. *Materials and Structures, 48*, 771–796, doi:10.1617/s11527-014-0515-0
39. Pundienė I., Kičaitė A., Pranckevičienė J. (2016): Impact of different types of plasticizing admixtures on the rheological properties and hydration of blended cements. *Journal of Thermal Analysis and Calorimetry,* 123, 1099-1109. doi: 10.1007/s10973-015-5020-3